Photoelectrochemistry

DOI: 10.1002/ange.201404697

A Tantalum Nitride Photoanode Modified with a Hole-Storage Layer for Highly Stable Solar Water Splitting**

*Guiji Liu, Jingying Shi, Fuxiang Zhang, Zheng Chen, Jingfeng Han, Chunmei Ding, Shanshan Chen, Zhiliang Wang, Hongxian Han, and Can Li**

Abstract: *Photoelectrochemical (PEC) water splitting is an ideal approach for renewable solar fuel production. One of the major problems is that narrow bandgap semiconductors, such as tantalum nitride, though possessing desirable band alignment for water splitting, suffer from poor photostability for water oxidation. For the first time it is shown that the presence of a ferrihydrite layer permits sustainable water oxidation at the tantalum nitride photoanode for at least 6 h with a benchmark photocurrent over 5 mA cm^{-2}, whereas the bare photoanode rapidly degrades within minutes. The remarkably enhanced photostability stems from the ferrihydrite, which acts as a hole-storage layer. Furthermore, this work demonstrates that it can be a general strategy for protecting narrow bandgap semiconductors against photocorrosion in solar water splitting.*

The direct conversion of solar energy to chemical fuels is not only of scientific interest but also a highly desirable approach to power the planet.[1] Photoelectrochemical (PEC) water splitting is a promising strategy for renewable solar fuel production using photoelectrodes.[2] However, trade-offs between light-harvesting and photostability of photoanodes have greatly limited the performance of PEC water splitting devices.[3] Typically, tantalum nitride (Ta_3N_5) has a desirable band alignment for water splitting and a theoretical solar to hydrogen conversion efficiency of 15.9%, but it is not stable in the highly oxidative environments of water oxidation.[4] To solve this problem, efforts have been made on alleviating accumulation of photogenerated holes by facilitating water oxidation.[5] For example, modification of Ta_3N_5 with IrO_2, an excellent water oxidation catalyst (WOC), could maintain half of the initial photocurrent in less than 10 min at 1.2 V versus the reversible hydrogen electrode (RHE).[5b,6] Recently, continuous production of oxygen in 100 min was reported on a cobalt phosphate (CoPi) WOC modified Ba-Ta_3N_5 photoanode at a moderate potential (0.9 V vs. RHE).[7] As yet, the endurance of the Ta_3N_5 photoanode in harsh oxidative environments for long-term performance still remains a challenging task.

Herein, for the first time, we employed a ferrihydrite (Fh) layer for protecting the unstable Ta_3N_5 photoanode against photocorrosion. With overlying Co_3O_4 nanoparticles (NPs), the resulting photoanode (designated as Co_3O_4/Fh/Ta_3N_5) yielded a photocurrent up to 5.2 mA cm^{-2} at a potential of 1.23 V vs. RHE under AM 1.5G simulated sunlight (100 mW cm^{-2}) and remained at about 94% of the initial activity after 6 h irradiation, which is the highest durability of the Ta_3N_5 based photoanodes reported to date.[5b,e]

The porous cubic Ta_3N_5 electrode shown in Figure 1a and b was formed by nitridation of $NaTaO_3$ film by an anodization and hydrothermal process on Ta substrate (Supporting Information, Figure S1) developed from our previous work.[8] The Ta_3N_5 electrode was then modified with a ferrihydrite layer (Figure 1c). The X-ray diffraction (XRD) pattern of the as-prepared ferrihydrite exhibits a poorly crystallized structure (Supporting Information, Figure S2), in agreement with previous reports.[9] The molecular formula of ferrihydrite

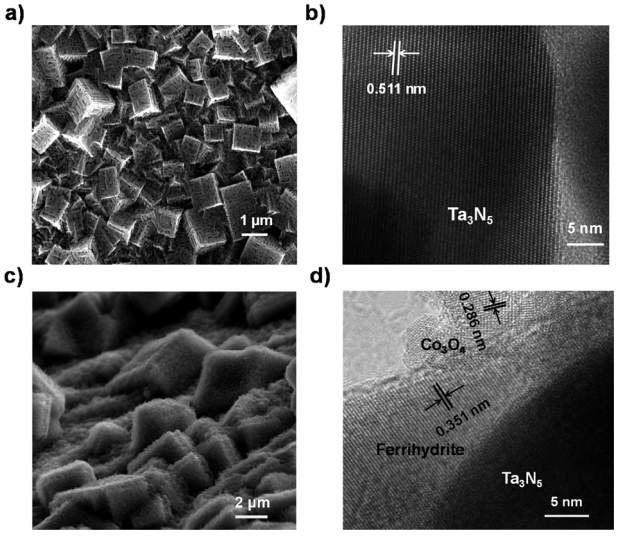

Figure 1. a) Scanning electron microscopy (SEM) image of bare Ta_3N_5 electrode (top view). b) High-resolution transmission electron micrograph (HRTEM) image of the as-prepared Ta_3N_5 film. c) SEM image of Fh/Ta_3N_5 electrode (side view). d) HRTEM image of Co_3O_4/Fh/Ta_3N_5 film.

[*] G. Liu,[+] Dr. J. Shi,[+] Prof. F. Zhang, Z. Chen, J. Han, C. Ding, S. Chen, Z. Wang, Prof. H. Han, Prof. C. Li
State Key Laboratory of Catalysis, Dalian Institute of Chemical Physics, Chinese Academy of Sciences
Dalian National Laboratory for Clean Energy
457 Zhongshan Road, Dalian 116023 (China)
E-mail: canli@dicp.ac.cn
Homepage: http://www.canli.dicp.ac.cn

[+] These authors contributed equally to this work.

[**] This work was financially supported by 973 National Basic Research Program of the Ministry of Science and Technology (No. 2014CB239400) and National Natural Science Foundation of China (No. 21090340, 21373210). F.Z. and H.H. acknowledge support by the "Hundred Talents Program" of the Chinese Academy of Sciences.

Supporting information for this article (including fabrication of Ta_3N_5 electrodes, ferrihydrite overlayers, and Co_3O_4 NPs) is available on the WWW under http://dx.doi.org/10.1002/anie.201404697.

is determined to be $Fe_5HO_8{\cdot}3H_2O$, based on thermogravimetric analysis (TGA) and X-ray photoelectron spectroscopic (XPS) results (Supporting Information, Figure S3). Subsequently, Co_3O_4 nanoparticles (NPs) were introduced by hydrothermal deposition to assemble Co_3O_4/Fh/Ta_3N_5 electrode (Figure 1 d).

Figure 2 a provides the current–potential curves of the above electrodes, including Co_3O_4/Ta_3N_5 for comparison. The addition of ferrihydrite mainly enhances the photocurrent of Ta_3N_5 at potentials lower than 1.40 V. In contrast, the introduction of Co_3O_4 NPs significantly increases the photocurrent of Ta_3N_5 over the entire potential range. Specifically, the photocurrent at the water oxidation potential (1.23 V) can reach up to 8.5 mA cm^{-2}, and the saturated photocurrent is almost 80% of its theoretical maximum photocurrent.[4b] Upon Co_3O_4 NPs, the Fh/Ta_3N_5 electrode exhibits a photocurrent of 5.2 mA cm^{-2} at 1.23 V, which is relatively low with respect to that of Co_3O_4/Ta_3N_5. This is most likely due to the ferrihydrite layer itself is in competition with the underlying Ta_3N_5 for light absorption (Supporting Information, Figure S4).

Figure 2 b shows stabilities of Ta_3N_5, Fh/Ta_3N_5, Co_3O_4/Ta_3N_5, and Co_3O_4/Fh/Ta_3N_5 electrodes for prolonged measurements at 1.23 V under AM 1.5 G simulated sunlight. The photocurrent of bare Ta_3N_5 electrode rapidly decays to a negligible level within minutes as the surface is oxidized (Supporting Information, Figure S5). The photostability of Co_3O_4/Ta_3N_5 electrode is still poor that only about 30% of the initial photocurrent remained after 2 h irradiation. Notably, the Fh/Ta_3N_5 electrode maintains about 90% of the initial value even after 6 h irradiation. The photocurrent enhancement, particularly at the beginning stage, is tentatively attributed to the "surface charging" process (Supporting Information, Figure S6) that requires further investigation. Moreover, the Co_3O_4 NPs decorated Fh/Ta_3N_5 electrode exhibits an initial photocurrent of over 5 mA cm^{-2} and remains about 94% of the initial activity after 6 h irradiation. To the best of our knowledge, photostability of Ta_3N_5-based systems at such high level of photocurrent within six hours has been barely achieved. Furthermore, continuous production of oxygen was found to occur at the Co_3O_4/Fh/Ta_3N_5 electrode for 12 h with Faraday efficiency of 96% (Supporting Information, Figure S7).

Although the detailed mechanism of the photocorrosion has not been well-understood, it is reported that the accumulated surface holes lead to the oxidative deactivation of Ta_3N_5.[5b,e] For this reason, the enhanced photostability of Ta_3N_5 is normally attributed to the efficient hole scavenge for water oxidation in previous reports.[5,7] However, we found that this is unlikely the primary reason for the improved photostability of ferrihydrite modified Ta_3N_5, based on the following experimental facts. As a hole scavenger, H_2O_2 was shown to be useful for assessing the performance of surface hole injection.[10] We therefore examined charge injection efficiencies of the Ta_3N_5, Fh/Ta_3N_5, Co_3O_4/Ta_3N_5, and Co_3O_4/Fh/Ta_3N_5 electrodes by comparing the photocurrent from water and H_2O_2 oxidation (Supporting Information, Figure S8). Figure 3 shows that the charge injection efficiency of Ta_3N_5 electrode is rather poor, indicating that photogenerated holes are initially accumulated on the surface. Once coupled with Co_3O_4 NPs, the charge injection efficiency of Ta_3N_5 is substantially enhanced, reaching 70% at a potential of 1.23 V. It is clear that the charge injection efficiency curve of Co_3O_4/Fh/Ta_3N_5 resembles that of Co_3O_4/Ta_3N_5 electrode, confirming that Co_3O_4 acts as an efficient WOC, which significantly promotes surface holes for water oxidation. On the contrary, both Fh/Ta_3N_5 and Ta_3N_5 electrodes possess similar low

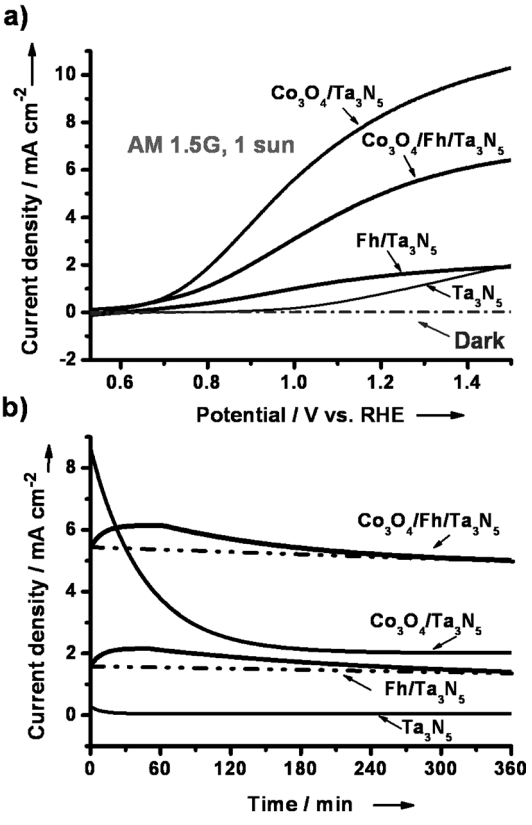

Figure 2. a) Current–potential curves of Ta_3N_5, Fh/Ta_3N_5, Co_3O_4/Ta_3N_5, and Co_3O_4/Fh/Ta_3N_5 photoanodes under AM 1.5 G simulated sunlight (100 mW cm^{-2}) in 1 M NaOH aqueous solution (pH 13.6). b) Chronoamperometry measurements of the above photoanodes at 1.23 V vs. RHE under AM 1.5 G simulated sunlight (100 mW cm^{-2}) in 1 M NaOH aqueous solution.

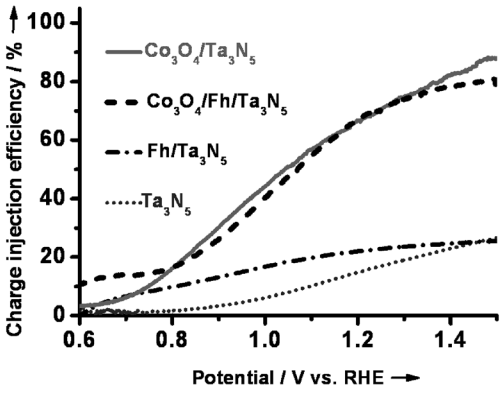

Figure 3. Charge injection efficiency versus potential curves of Ta_3N_5, Fh/Ta_3N_5, Co_3O_4/Ta_3N_5, and Co_3O_4/Fh/Ta_3N_5 photoanodes.

charge-injection efficiencies at 1.23 V, implying a relatively poor catalytic nature for water oxidation. These results suggest that there exists a different mechanism for the superior photostability of ferrihydrite-modified Ta_3N_5 electrodes.

To gain more insight into the principle of this situation, we investigated the electrochemical behavior of ferrihydrite film on fluorine-doped tin oxide (FTO) substrate. The Mott–Schottky (MS) analysis is shown in Figure 4a, divided into three sections according to the different variations of capacitance versus potential. In section 1, it exhibits linear dependence with a positive slope, which is a typical feature for an n-type semiconductor. In section 2, the semiconductor capacitance is stabilized, which is associated with the surface redox states charging as discussed in previous reports for α-Fe_2O_3 and TiO_2.[11] The energy levels of the surface redox states can be obtained from the derivative of the plot in section 2,[11b] which are closed to each other forming into a potential gradient for capturing charges (Supporting Information, Figure S9). In section 3, a linear dependence with a negative slope reflects that a positively charged inversion layer is formed after these surface states are emptied, indicating that holes might be stored. Galvanostatic charge–discharge measurement further confirms that holes can be stored at the ferrihydrite in the form of positively charged states, although some of them seem to be "lost" prior to be discharged (Supporting Information, Figure S10).

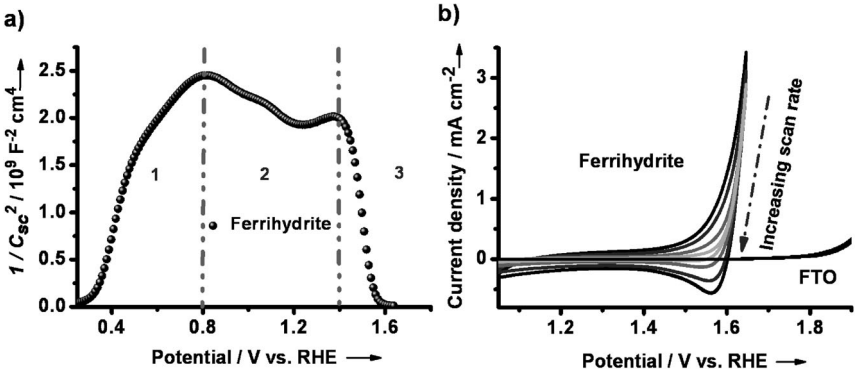

Figure 4. a) MS plot of ferrihydrite film on FTO with the AC potential frequency of 1000 Hz. b) CV diagrams for ferrihydrite film on FTO under scan rates of 10–100 $mV s^{-1}$ with three cycles.

To understand this phenomenon, we performed cyclic voltammogram (CV) for ferrihydrite. Figure 4b shows that the appearance of water oxidation current is coincided with the built-up of hole storage. The electrochemical impedance spectroscopy (EIS) further reveals that the decrease of charge-transfer resistance is correlated to the increase of corresponding capacitance (Supporting Information, Figure S11). These results suggest that once a critical number of holes are accumulated, water oxidation progresses.[12] As a result, some stored holes appear "lost" for water oxidation, while the additional undergo discharging, evidenced by the observation of a cathodic capacitive peak at 1.55 V[13] (a linear scan rate dependence of peak current is present in the Supporting Information, Figure S12). The presence of hole storage on ferrihydrite is most likely due to the hole transfer to water is lower than hole entering, as no cathodic current was measured in solution containing H_2O_2 (Supporting Information, Figure S13).

Given the above findings, it is reasonable to deduce that photogenerated holes of Ta_3N_5 could be captured and stored at ferrihydrite in a similar manner. Following this inference, charge transport of Ta_3N_5 could be promoted by ferrihydrite.[14] Indeed, the charge separation curve of Fh/Ta_3N_5 exhibits a better fill factor than that of Ta_3N_5 electrode (Supporting Information, Figure S14). Another interesting feature is that evident transient anodic/cathodic peaks appear upon light on/off, when ferrihydrite is added (Supporting Information, Figure S15). This phenomenon indicates that surface-reaching holes are initially stored, which in turn increase a recombination flux of electrons to the surface.[11a,15] A plot of the stored charge is also shown in Figure 5a, calculated from chronoamperometry measurements (Supporting Information, Figure S16). It is striking that charge storage of Ta_3N_5 is increased by at least two orders of magnitude owing to the addition of ferrihydrite. More interestingly, the

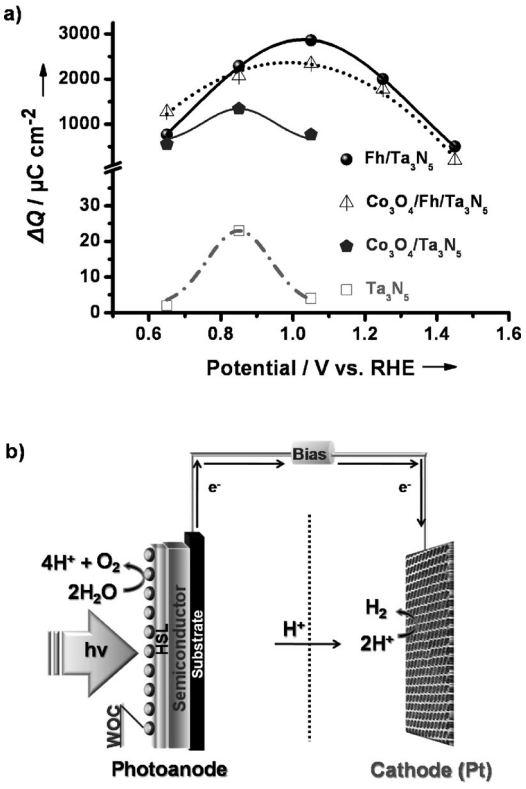

Figure 5. a) Charge storage versus potential curves of Ta_3N_5, Fh/Ta_3N_5, Co_3O_4/Ta_3N_5, and $Co_3O_4/Fh/Ta_3N_5$ photoanodes. b) Representation of the HSL approach for solar water splitting.

order of charge storage capacity agrees well with the photostability of these photoanodes (Figure 2b) that the one with higher level of charge storage can be resistant to the photocorrosion. As previously mentioned, Fh/Ta_3N_5 and Ta_3N_5 undergo the same situation that holes are initially accumulated at the surface; however, Fh/Ta_3N_5 exhibits superior photostability. This led us to consider that the charge storage capacity might be a dominant factor for the photostability of Ta_3N_5.

To verify this conclusion, we used H_2O_2 to represent a "WOC" with ultimate performance of consuming surface holes for oxygen evolution, but limited capacity of charge storage. It turns out that an apparent photocurrent decay of Ta_3N_5 can be observed even with this excellent "WOC" (Supporting Information, Figure S17). In light of this, charge storage capacity might be an indispensable factor for maintaining the stability of Ta_3N_5 electrode. An additional confirmation is that the stability of electrode under potentials, where charge storage is still evident, seems better than that under potentials with limited charge storage (Supporting Information, Figure S18). Based on the above analysis, the improved stability of Ta_3N_5 electrode is very likely related to the increased charge storage capacity, stemming from ferrihydrite.

Among reports on Fe-based oxyhydroxides for water splitting, Choi et al. demonstrated that γ-FeOOH is an efficient WOC for $BiVO_4$ electrode.[16] Mullins et al. also showed that an amorphous FeOOH is a promising WOC for PEC water splitting.[17] The ferrihydrite herein, however, appears to have distinct properties with those previous works. Thus, we propose that the essential role of ferrihydrite is a hole-storage layer (HSL) that affords the unstable semiconductor (Ta_3N_5) for sustainable solar water splitting, as shown in Figure 5b.

We next applied the HSL approach for protecting unstable oxynitrides (TaON) and oxides ($BiVO_4$; Supporting Information, Figure S19). The photocurrent of the bare TaON and $BiVO_4$ photoanodes decrease dramatically within a few minutes, but the addition of ferrihydrite extends the durability of these photoanodes to hours for continuous water oxidation. Theses representative examples further demonstrate the general applicability of the HSL strategy in preventing unstable semiconductors from photocorrosion.

In summary, we have introduced the concept of HSL, using ferrihydrite, whereby photogenerated holes of Ta_3N_5 can be captured and stored, allowing sustainable water oxidation at the otherwise unstable Ta_3N_5 photoanode for at least 6 h. To the best of our knowledge, this is the most durable Ta_3N_5 based photoanode against photocorrosion reported so far. More importantly, we found that the charge storage capacity might be critical for the photostability of Ta_3N_5, which can offer a new insight into photocorrosion encountered in water oxidation. Efforts are being made on in-depth understanding of the mechanism in the HSL system for solar water splitting. We believe that the proof-of-principle work described herein demonstrates the general applicability of this approach, opening up a new avenue for developing efficient and stable photoelectrodes in the field of renewable solar fuel production.

Received: April 25, 2014
Published online: May 30, 2014

Keywords: electrochemistry · ferrihydrite · photochemistry · tantalum nitride · water splitting

[1] a) N. S. Lewis, *Science* **2007**, *315*, 798 – 801; b) X. Chen, C. Li, M. Gratzel, R. Kostecki, S. S. Mao, *Chem. Soc. Rev.* **2012**, *41*, 7909 – 7937.

[2] a) A. Fujishima, K. Honda, *Nature* **1972**, *238*, 37 – 38; b) A. J. Bard, *Science* **1980**, *207*, 139 – 144; c) M. Grätzel, *Nature* **2001**, *414*, 338 – 344.

[3] a) M. G. Walter, E. L. Warren, J. R. McKone, S. W. Boettcher, Q. Mi, E. A. Santori, N. S. Lewis, *Chem. Rev.* **2010**, *110*, 6446 – 6473; b) S. Y. Chen, L. W. Wang, *Chem. Mater.* **2012**, *24*, 3659 – 3666.

[4] a) W. J. Chun, A. Ishikawa, H. Fujisawa, T. Takata, J. N. Kondo, M. Hara, M. Kawai, Y. Matsumoto, K. Domen, *J. Phys. Chem. B* **2003**, *107*, 1798 – 1803; b) A. B. Murphy, P. R. F. Barnes, L. K. Randeniya, I. C. Plumb, I. E. Grey, M. D. Horne, J. A. Glasscock, *Int. J. Hydrogen Energy* **2006**, *31*, 1999 – 2017; c) A. Ishikawa, T. Takata, J. N. Kondo, M. Hara, K. Domen, *J. Phys. Chem. B* **2004**, *108*, 11049 – 11053.

[5] a) Y. Q. Cong, H. S. Park, S. J. Wang, H. X. Dang, F. R. F. Fan, C. B. Mullins, A. J. Bard, *J. Phys. Chem. C* **2012**, *116*, 14541 – 14550; b) M. J. Liao, J. Y. Feng, W. J. Luo, Z. Q. Wang, J. Y. Zhang, Z. S. Li, T. Yu, Z. G. Zou, *Adv. Funct. Mater.* **2012**, *22*, 3066 – 3074; c) Y. Li, T. Takata, D. Cha, K. Takanabe, T. Minegishi, J. Kubota, K. Domen, *Adv. Mater.* **2013**, *25*, 125 – 131; d) C. Zhen, L. Wang, G. Liu, G. Q. Lu, H. M. Cheng, *Chem. Commun.* **2013**, *49*, 3019 – 3021; e) J. Hou, Z. Wang, C. Yang, H. Cheng, S. Jiao, H. Zhu, *Energy Environ. Sci.* **2013**, *6*, 3322 – 3330; f) M. Li, W. Luo, D. Cao, X. Zhao, Z. Li, T. Yu, Z. Zou, *Angew. Chem.* **2013**, *125*, 11222 – 11226; *Angew. Chem. Int. Ed.* **2013**, *52*, 11016 – 11020.

[6] D. Yokoyama, H. Hashiguchi, K. Maeda, T. Minegishi, T. Takata, R. Abe, J. Kubota, K. Domen, *Thin Solid Films* **2011**, *519*, 2087 – 2092.

[7] Y. Li, L. Zhang, A. Torres-Pardo, J. M. Gonzalez-Calbet, Y. Ma, P. Oleynikov, O. Terasaki, S. Asahina, M. Shima, D. Cha, L. Zhao, K. Takanabe, J. Kubota, K. Domen, *Nat. Commun.* **2013**, *4*, 2566.

[8] J. Y. Shi, G. J. Liu, N. Wang, C. Li, *J. Mater. Chem.* **2012**, *22*, 18808 – 18813.

[9] a) J. L. Jambor, J. E. Dutrizac, *Chem. Rev.* **1998**, *98*, 2549 – 2586; b) F. M. Michel, L. Ehm, S. M. Antao, P. L. Lee, P. J. Chupas, G. Liu, D. R. Strongin, M. A. Schoonen, B. L. Phillips, J. B. Parise, *Science* **2007**, *316*, 1726 – 1729; c) F. M. Michel, V. Barron, J. Torrent, M. P. Morales, C. J. Serna, J. F. Boily, Q. Liu, A. Ambrosini, A. C. Cismasu, G. E. Brown, Jr., *Proc. Natl. Acad. Sci. USA* **2010**, *107*, 2787 – 2792.

[10] a) H. Dotan, K. Sivula, M. Gratzel, A. Rothschild, S. C. Warren, *Energy Environ. Sci.* **2011**, *4*, 958 – 964; b) D. K. Zhong, S. Choi, D. R. Gamelin, *J. Am. Chem. Soc.* **2011**, *133*, 18370 – 18377.

[11] a) B. Klahr, S. Gimenez, F. Fabregat-Santiago, J. Bisquert, T. W. Hamann, *Energy Environ. Sci.* **2012**, *5*, 7626 – 7636; b) M. Tomkiewicz, *J. Electrochem. Soc.* **1979**, *126*, 1505 – 1510.

[12] a) B. Klahr, S. Gimenez, F. Fabregat-Santiago, T. Hamann, J. Bisquert, *J. Am. Chem. Soc.* **2012**, *134*, 4294 – 4302; b) R. L. Doyle, M. E. Lyons, *Phys. Chem. Chem. Phys.* **2013**, *15*, 5224 – 5237.

[13] L. Bertoluzzi, L. Badia-Bou, F. Fabregat-Santiago, S. Gimenez, J. Bisquert, *J. Phys. Chem. Lett.* **2013**, *4*, 1334 – 1339.

[14] a) J. A. Seabold, K. S. Choi, *Chem. Mater.* **2011**, *23*, 1105 – 1112; b) B. Klahr, S. Gimenez, F. Fabregat-Santiago, J. Bisquert, T. W. Hamann, *J. Am. Chem. Soc.* **2012**, *134*, 16693 – 16700.

[15] a) F. Le Formal, K. Sivula, M. Grätzel, *J. Phys. Chem. C* **2012**, *116*, 26707 – 26720; b) L. M. Peter, *J. Solid State Electrochem.* **2013**, *17*, 315 – 326.
[16] a) J. A. Seabold, K. S. Choi, *J. Am. Chem. Soc.* **2012**, *134*, 2186 – 2192; b) K. J. McDonald, K. S. Choi, *Energy Environ. Sci.* **2012**, *5*, 8553 – 8557; c) T. W. Kim, K. S. Choi, *Science* **2014**, *343*, 990 – 994.
[17] W. D. Chemelewski, H. C. Lee, J. F. Lin, A. J. Bard, C. B. Mullins, *J. Am. Chem. Soc.* **2014**, *136*, 2843 – 2850.

